Received: 18 May 2023 | Revised: 30 November 2023 | Accepted: 1 December 2023

DOI: 10.1111/jace.19702

Journal of the American Ceramic Society

RESEARCH ARTICLE

Solid state synthesis of $BiFeO_3$ occurs through the intermediate $Bi_{25}FeO_{39}$ compound

Corrado Wesley[1] | **Leah Bellcase**[1] | **Jennifer S. Forrester**[2] | **Elizabeth C. Dickey**[3] | **Ian M. Reaney**[4] | **Jacob L. Jones**[1]

[1]Department of Materials Science and Engineering, North Carolina State University, Raleigh, North Carolina, USA

[2]Analytical Instrumentation Facility, North Carolina State University, Raleigh, North Carolina, USA

[3]Department of Materials Science and Engineering, Carnegie Mellon University, Pittsburgh, Pennsylvania, USA

[4]Department of Materials Science and Engineering, University of Sheffield, Sheffield, UK

Correspondence
Corrado Wesley and Jacob L. Jones, Department of Materials Science, North Carolina State University, Raleigh, NC 27695, USA.
Email: corradojh@gmail.com and jljone21@ncsu.edu

Funding information
Center for Dielectrics and Piezoelectrics, North Carolina State University, Grant/Award Numbers: ECCS-2025064, IIP-1841453, IIP-1841466

Abstract

The solid-state synthesis of perovskite $BiFeO_3$ has been a topic of interest for decades. Many studies have reported challenges in the synthesis of $BiFeO_3$ from starting oxides of Bi_2O_3 and Fe_2O_3, mainly associated with the development of persistent secondary phases such as $Bi_{25}FeO_{39}$ (sillenite) and $Bi_2Fe_4O_9$ (mullite). These secondary phases are thought to be a consequence of unreacted Fe-rich and Bi-rich regions, that is, incomplete interdiffusion. In the present work, in situ high-temperature X-ray diffraction is used to demonstrate that Bi_2O_3 first reacts with Fe_2O_3 to form sillenite $Bi_{25}FeO_{39}$, which then reacts with the remaining Fe_2O_3 to form $BiFeO_3$. Therefore, the synthesis of perovskite $BiFeO_3$ is shown to occur via a two-step reaction sequence with $Bi_{25}FeO_{39}$ as an intermediate compound. Because $Bi_{25}FeO_{39}$ and the γ-Bi_2O_3 phase are isostructural, it is difficult to discriminate them solely from X-ray diffraction. Evidence is presented for the existence of the intermediate sillenite $Bi_{25}FeO_{39}$ using quenching experiments, comparisons between Bi_2O_3 behavior by itself and in the presence of Fe_2O_3, and crystal structure examination. With this new information, a proposed reaction pathway from the starting oxides to the product is presented.

KEYWORDS
ferrites, ferroelectricity/ferroelectric materials, perovskites, synthesis, X-ray methods

1 | INTRODUCTION

$BiFeO_3$ is a scientifically and industrially interesting ferroic oxide because it can exhibit both antiferromagnetic and ferroelectric properties. The synthesis of $BiFeO_3$ is typically undertaken by solid-state reaction of the starting oxides of Bi_2O_3 and Fe_2O_3 in the region of 750°C,[1] although techniques such as wet chemical and sol–gel methods have been explored with some success.[2,3] Although the solid-state reaction of $BiFeO_3$ from Bi_2O_3 and Fe_2O_3 is simple in chemical formula, significant complications and challenges have been reported.

A description of solid-state synthesis was outlined by Bernardo et al.[4] in which it was proposed that the Bi_2O_3 diffuses into the Fe_2O_3 particle, which then forms $BiFeO_3$. This schematic diagram is reproduced in Figure 1. In Figure 1, the idealized final stage of the reaction is shown with the arrow toward the top-right of the figure, a process

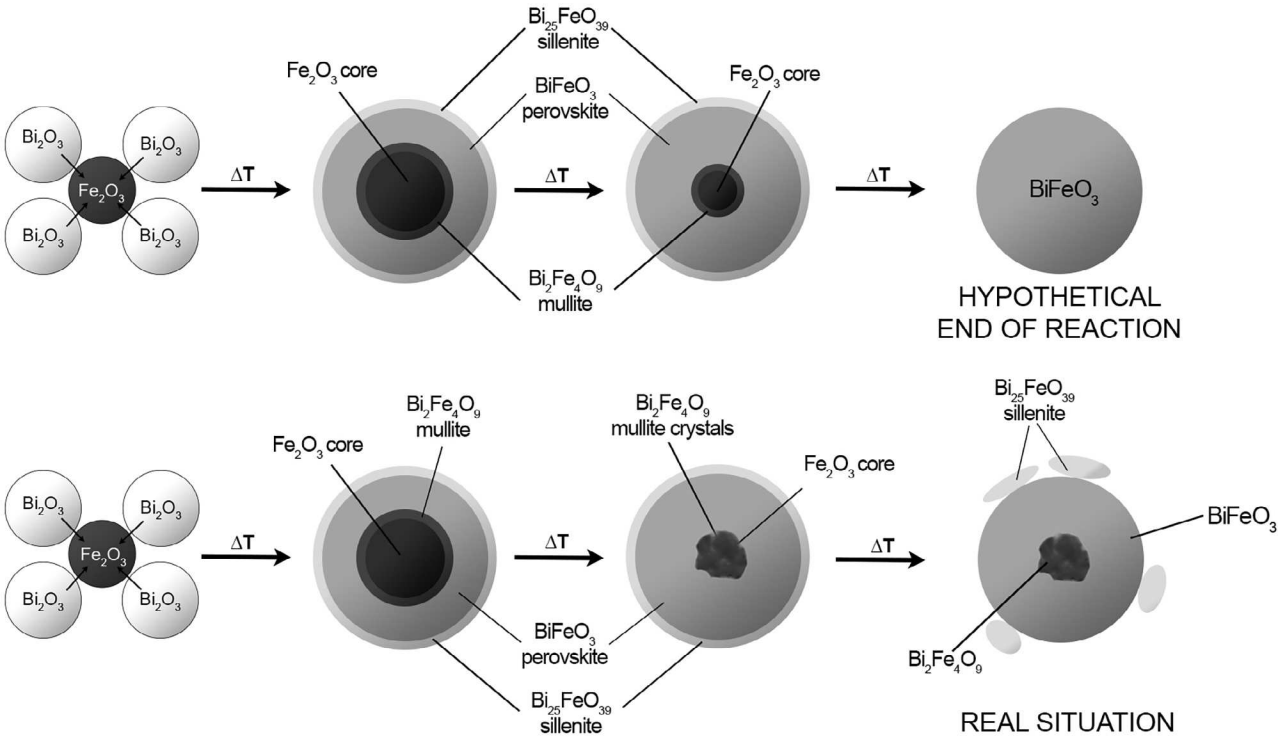

FIGURE 1 The reaction pathway for Bi_2O_3–Fe_2O_3 to $BiFeO_3$ redrawn after and adapted from Bernardo et al.[4]

resulting in homogeneous $BiFeO_3$. However, interdiffusion is required between Bi_2O_3 and Fe_2O_3, which allows other, undesirable compounds to form, and the chemical gradient can result in a core-shell structure. With diffusion of Bi_2O_3 into the Fe_2O_3 particle, the initial core of Fe_2O_3 evolves to an iron-rich $Bi_2Fe_4O_9$ (mullite) phase, which is a line compound, leaving the shell Fe-deficient. Some $BiFeO_3$ develops, with remaining Bi-rich material forming $Bi_{25}FeO_{39}$ (sillenite) phase, another line compound. Bi^{3+} and Fe^{3+} from the precursor are trapped within these secondary phases, inhibiting further reaction to form the perovskite phase.

It is also important to note that $BiFeO_3$ is a line compound itself. A phase diagram is given in Palai et al.[5] showing that if the composition deviates from this line, then secondary phases such as sillenite and mullite become favorable. Valant et al.[6] further emphasized that these secondary phases are thermodynamically favorable and are further stabilized by the presence of impurities.

While Fe_2O_3 is not expected to exhibit polymorphic phase transitions within the formation temperature of $BiFeO_3$, Bi_2O_3 is monoclinic (designated α-Bi_2O_3) at room temperature and undergoes polymorphic phase transitions on heating,[5] which possibly influences the reaction. Reported phases in Bi_2O_3 include monoclinic α-Bi_2O_3, face-centered cubic (fcc) δ-Bi_2O_3 (the high temperature cubic phase), and body-centered cubic (bcc) γ-Bi_2O_3 (a metastable cubic phase).[5] However, there is no consensus on the phase transitions occurring during the reaction to form $BiFeO_3$ and their role in the synthesis itself. Morozov et al.[7] reported that the α-Bi_2O_3 phase converts to the γ-Bi_2O_3 at approximately 730°C. Thrall et al.[8] using in situ high-temperature X-ray diffraction (HTXRD), reported that α-Bi_2O_3 converts to γ-Bi_2O_3 at approximately 650–700°C under vacuum and inert environments. However, previous reports suggest that α-Bi_2O_3 converts to δ-Bi_2O_3 at 730°C, and that γ-Bi_2O_3 is only observed during cooling from the higher temperature δ-Bi_2O_3 phase.[9–11]

There is evidence in the literature that between 447 and 767°C, $BiFeO_3$ is metastable, and decomposes into thermodynamically stable secondary phases, often with remaining starting oxides present.[1] A study by Selbach et al.[12] showed that $BiFeO_3$ decomposed to secondary phases between 600 and 900°C, and then re-formed $BiFeO_3$ at higher temperatures. Morozov et al.[7] claimed that $BiFeO_3$ always yields other compounds as impurities. These results evidence the challenges of synthesizing pure-phase $BiFeO_3$ using solid-state reactions.

Understanding the reaction fully requires the in situ identification of phases, which is most appropriate for X-ray diffraction (XRD). However, a central challenge in following the phase evolution during the synthesis of $BiFeO_3$ using XRD is that metastable γ-Bi_2O_3 is isostructural to $Bi_{25}FeO_{39}$[13,14]; consequently, the XRD patterns of the two phases are difficult to distinguish from one another. However, there exist various approaches for

discerning the phases. One approach is to closely examine the cell metrics. For example, Levin and Roth[15] reported that the lattice parameters of an undoped, metastable bcc phase of Bi_2O_3 are much larger than a distinct, stable bcc phase of Bi_2O_3 with Fe_2O_3 incorporation. Figure S1[15] in Supporting Information shows the expected lattice parameters. Of relevance to the current work is the undoped, metastable bcc phase of Bi_2O_3 lattice parameter of 10.27 Å, and the distinct, stable bcc phase of approximately 4 mol% Fe_2O_3-modified Bi_2O_3, which is approximately 10.19 Å. These lattice parameters are referenced further in the following sections.

To provide insight into the solid-state reaction of Bi_2O_3 and Fe_2O_3 to form $BiFeO_3$, several in situ HTXRD experiments are presented. In situ HTXRD experiments include heating and cooling the starting oxides individually at multiple heating rates in air, heating and cooling mixed starting oxides to form $BiFeO_3$, and partially heating mixed starting oxides that were quenched. These experiments demonstrate that all the Bi_2O_3 reacts with a small amount of Fe_2O_3 to form sillenite $Bi_{25}FeO_{39}$ prior to the formation of $BiFeO_3$. In other words, the reaction of Bi_2O_3 with Fe_2O_3 to form $BiFeO_3$ occurs via a two-step reaction sequence with sillenite $Bi_{25}FeO_{39}$ as the intermediate compound.

2 | EXPERIMENTAL PROCEDURES

Starting powders of Bi_2O_3 (99.99%, Alfa Aesar) and Fe_2O_3 (99.99%, Alfa Aesar) were weighed in equimolar proportions to target the formation of $BiFeO_3$. All experiments involved ball milling of the powders prior to HTXRD in ethanol for 24 h using 10 mm yttria stabilized zirconia milling media (20:1). No milling media contamination was observed in the products after the milling process. A scanning electron microscope (SEM) image of the milled powder is provided in Figure S2 and shows that the Bi_2O_3 and Fe_2O_3 particles are on the scale of approximately 1 μm and 100 nm, respectively. All powders were heated in an Anton Paar XRK 900 reaction chamber with z-stage automated alignment while mounted in a PANalytical Empyrean powder diffractometer with Cu Kα radiation under an ambient gas with a heating rate of 1°C/min. In situ HTXRD patterns were measured continuously in a 2θ range of 20°–80° using a step size of 0.026°. In situ patterns were also measured during cooling at a rate of 10°C/min.

3 | RESULTS AND DISCUSSION

An important aspect of this work is to identify the role of the phase transitions in Bi_2O_3 in the synthesis of $BiFeO_3$. It is therefore critical to differentiate between the isostructural phases of γ-Bi_2O_3 and $Bi_{25}FeO_{39}$. With that in mind, the phase transitions in Bi_2O_3 when heated by itself to 780°C at 1°C/min, held at that temperature for 1 h, then cooled at 10°C/min to room temperature are determined and these results are presented in Figure 2A. Figure S3 shows these results over a wider 2θ range. Fe_2O_3 was heat treated under the same conditions, though there were no phase transitions observed (results not shown here).

The in situ HTXRD scan in Figures 2A and S3 shows that when α-Bi_2O_3 is heated by itself, the initial monoclinic α-Bi_2O_3 persists to between 700 and 750°C, at which temperature it transitions to fcc δ-Bi_2O_3. On cooling, the δ-Bi_2O_3 converts to γ-Bi_2O_3, which is consistent with Harwig and Gerards[11] and Levin and Roth.[15] In the present study as well as in the works of Harwig and Gerards[11] and Levin and Roth,[16] the γ-Bi_2O_3 phase is only observed during cooling. At approximately 500°C during cooling, the γ-Bi_2O_3 transitions to α-Bi_2O_3, demonstrating reversibility to the original phase upon cooling. In other experiments not shown here, milled α-Bi_2O_3 powders were heated at 1°C/min and unmilled α-Bi_2O_3 was heated at 5°C/min, and the same phase transitions were observed, showing the persistence of this observation with different sample preparation methods and heating rates. The observation that γ-Bi_2O_3 is not present on heating is discussed later in the manuscript in relation to the reactions to form $BiFeO_3$.

To synthesize $BiFeO_3$, an equimolar mixture of milled Bi_2O_3 and Fe_2O_3 was heated to 780°C, a temperature, determined from iterative experiments, which enabled full reaction to form $BiFeO_3$. The HTXRD measurements of the full reaction to form $BiFeO_3$ are shown in Figure 2B. Figure S4 shows these results over a wider 2θ range.

There are several features to highlight in the in situ HTXRD measurements in Figures 2B and S4. First, all the α-Bi_2O_3 converts into a different crystal structure at approximately 600°C. In Figure 2A, α-Bi_2O_3 by itself does not appear to change phase until approximately 750°C, at which temperature it converts to δ-Bi_2O_3. The comparison of this initial observation (in Figure 2B) to that of Bi_2O_3 heated by itself (Figure 2A) indicates a possible phase transition and/or an intermediate phase. More specifically, that Fe causes this intermediate phase, suggests that it is likely sillenite, $Bi_{25}FeO_{39}$, rather than γ-Bi_2O_3. Another important observation in Figure 2B is that $BiFeO_3$ starts to form at approximately 700°C, before the $Bi_{25}FeO_{39}$ phase has completely disappeared. As the sillenite phase disappears, mullite forms and persists through the entire thermal process. The mullite phase peak positions agree with positions reported previously in literature.[1] With continued heating, the remainder of the Fe_2O_3 reacts with the sillenite to form $BiFeO_3$. On cooling (Figure 2B), the $BiFeO_3$ product remains.

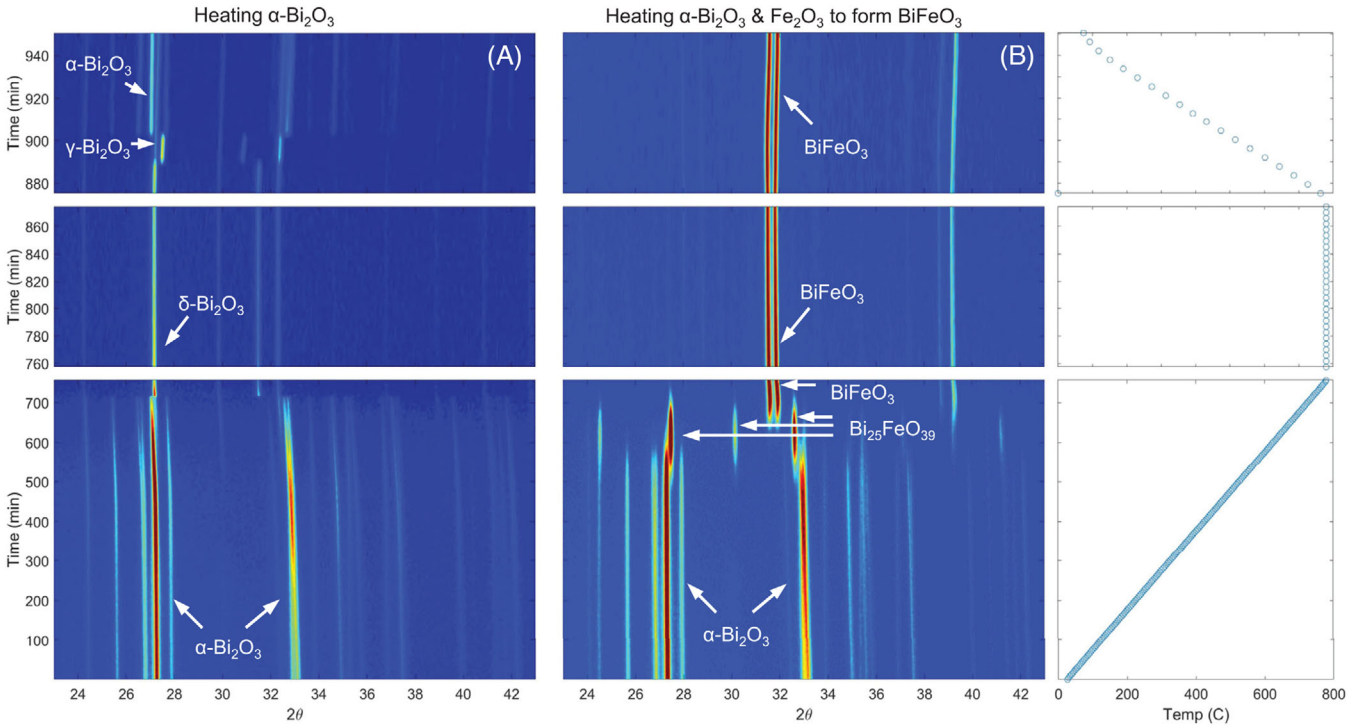

FIGURE 2 Powder diffraction patterns measured in situ during high-temperature X-ray diffraction (HTXRD) of (A) Bi_2O_3 heating and cooling by itself, and (B) Bi_2O_3 and Fe_2O_3 heated to react and form $BiFeO_3$.

In the specific experiment shown in Figure 2B, the persistence of a very minor fraction of $Bi_2Fe_4O_9$ is a reminder of the importance of starting particle size, as can be inferred from Figure 1. By repeating this experiment multiple times, examples can be found where the final products are phase-pure $BiFeO_3$ within the resolution limits of diffraction. The variability in the final phase is a consequence of the small quantities of powders used in the HTXRD experiment and their state of mixing when placed on the heating stage. An indexed pattern of a resulting phase-pure $BiFeO_3$ in one of these experiments is shown in Figure 3.

Another important observation that needs to be informed for understanding of the reaction sequence is the behavior of the Fe_2O_3 diffraction peaks. The intensity of Bi_2O_3 is much higher than that of Fe_2O_3 (mostly attributed to the difference in atomic scattering factors of Bi vs. Fe), meaning that most of the reflections in the lower 2θ region of Figure 2B are assigned to Bi_2O_3. The major peaks of the initial rhombohedral Fe_2O_3 phase (PDF pattern 04-015-6947) are at 2θ approximately 24.15° (012 reflection), and at 2θ approximately 33.16° (104 reflection), which lies in the same 2θ range as α-Bi_2O_3 122/200. To illustrate the reaction sequence more closely, a magnified section of Figure 2B is included as shown in Figure 4.

Figure 4 shows that the α-Bi_2O_3 (peak at approximately 21.7° 2θ) disappears by approximately 545°C, much lower than the beginning of $BiFeO_3$ formation. The disappearance of the α-Bi_2O_3 peak does, however, coincide with the appearance of the peak at approximately 21.1° 2θ (which could be assigned to either $Bi_{25}FeO_{39}$ or γ-Bi_2O_3). The Fe_2O_3 (peak at approximately 21.1° 2θ) persists to at least 100°C higher than the α-Bi_2O_3. The peak at approximately 24.5° 2θ is initially α-Bi_2O_3, and then intensifies, which appears to be a major peak of the intermediate phase. The persistence of the peak at approximately 24.5° 2θ suggests a crystallographic relationship between the α-Bi_2O_3 and the intermediate phase ($Bi_{25}FeO_{39}$ or γ-Bi_2O_3).

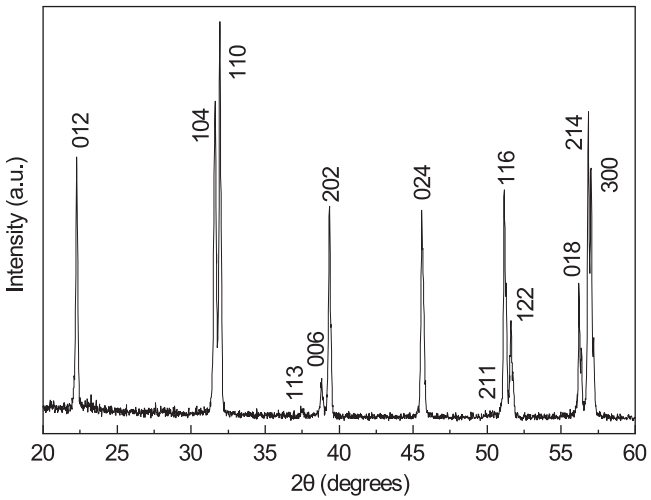

FIGURE 3 Indexed diffraction pattern of $BiFeO_3$ resulting from a high-temperature X-ray diffraction (HTXRD) experiment.

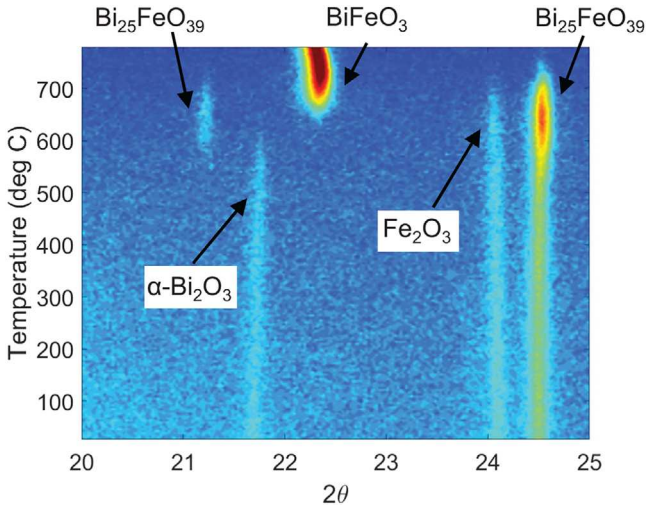

FIGURE 4 Magnified view of Figure 2 in the 2θ range of 20°–25°C.

To further study the intermediate phase, a separate in situ reaction was performed and quenched with the aim of locking in the intermediate phase ($Bi_{25}FeO_{39}$ or γ-Bi_2O_3), for example, to examine (ir)reversibility of the phase transitions. The experiment involved heating equimolar Bi_2O_3 and Fe_2O_3 at a 1°C/min heating rate to 650°C, then cooled at 20°C/min to room temperature. The result of this experiment is shown in Figure 5A. Multiple room temperature XRD patterns are recorded over several days following the experiment and a representative pattern is shown in Figure 5B.

Figure 5A shows that the intermediate phase appears at the times and temperatures expected relative to that shown earlier in Figure 2B. After quenching from 650°C to room temperature, the intermediate phase persists, as shown in Figure 5B. Referring to the experiment involving heating of Bi_2O_3 by itself (Figure 2A), if the intermediate phase is metastable γ-Bi_2O_3, it should revert to α-Bi_2O_3 on cooling. However, the room temperature XRD patterns after quenching (e.g., Figure 5B) show the persistence of sillenite $Bi_{25}FeO_{39}$ for several days after the experiment. The phases present at room temperature after the interrupted reaction are $Bi_{25}FeO_{39}$, Fe_2O_3, and a minor fraction of $BiFeO_3$. Most importantly, no α-Bi_2O_3 remains after cooling. The persistence of the intermediate phase after cooling proves that it is not γ-Bi_2O_3 and is consistent with the formation of $Bi_{25}FeO_{39}$.

The quenched powders are also investigated using transmission electron microscopy with energy-dispersive spectroscopy (EDS) and representative images are shown in Figure 6. The EDS maps show two distinct regions which are consistent with the XRD observations: (i) regions "1" are from the larger of two particle sizes which are Bi-rich with a small amount of Fe distributed homogeneously throughout, consistent with the sillenite phase, and (ii) regions "2" are from the smaller particle size which are Fe-rich with no Bi, consistent with Fe_2O_3. These two types of particles are commensurate with the results from XRD, which shows a mixture of $Bi_{25}FeO_{39}$ and Fe_2O_3.

Since Figure 6 illustrates that Fe has diffused homogeneously throughout the particles that were originally Bi_2O_3, it is natural to question whether larger particles of Bi_2O_3 would still react with the Fe_2O_3 to form sillenite, given that they require longer diffusion lengths. To test whether sillenite forms when starting with larger particles, Bi_2O_3 was intentionally coarsened to increase the grain size, using a heating rate of 1°C/min, a hold at 650°C for 2 h, and then cooling at a rate of 5°C/min. The coarsened Bi_2O_3 particles were then combined with equimolar Fe_2O_3 and heated in the diffractometer. The HTXRD results, reported in Figure S5, show that the sillenite phase occurs in parallel to the disappearance of the Bi_2O_3 phase. With further heating, the sillenite reacts with Fe_2O_3 to form $BiFeO_3$, and some sillenite phase is retained in the final pattern. Fe can, therefore, still diffuse into larger Bi_2O_3 particles, forming sillenite during the reaction. SEM images and EDS maps of the starting particles and the final products of this experiment are shown in Figure S6. The SEM images and EDS maps are consistent with the HTXRD results, showing that some $BiFeO_3$ forms while the larger particles exacerbate the persistence of the sillenite phase.

Data from the XRD pattern shown in Figure 5B are used to refine crystal structure models using the Rietveld method. The XRD pattern was modeled using either the $Bi_{25}FeO_{39}$ phase or the γ-Bi_2O_3 phase. Although the final phase is already proven through the quenching study to not be γ-Bi_2O_3, we nevertheless model this phase to compare to the work of Levin and Roth.[15] Both calculated patterns fitted the experimental pattern well, with Bragg R factors of approximately 4%. The refinement using $Bi_{25}FeO_{39}$ resulted in marginally better fit parameters, however it was not sufficiently better that it could be used as a basis for determining which phase is present, demonstrating the need for complementary experiments, such as heating of the powders independently (e.g., Figure 2A). Figure S7 shows the results of this refinement when using $Bi_{25}FeO_{39}$ as the major phase which was used to obtain the cubic unit cell parameter. The refined lattice parameter is 10.1876(3) Å which matches the distinct, stable bcc phase of Bi_2O_3 with Fe_2O_3 incorporation (~10.18 Å) in Figure S1,[15] better than Bi_2O_3 (~10.27 Å), supporting the presence of the intermediate phase, $Bi_{25}FeO_{39}$.

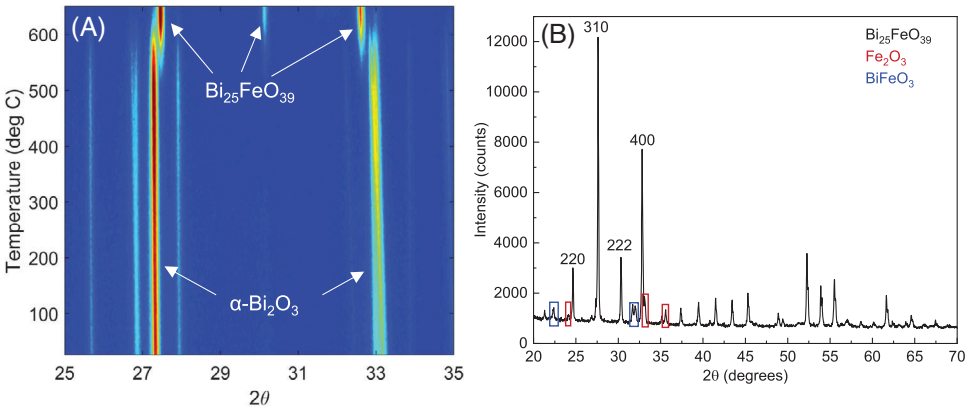

FIGURE 5 (A) Powder diffraction patterns measured in situ during high-temperature X-ray diffraction (HTXRD) of Bi_2O_3 with Fe_2O_3 up to 650°C, after which the sample was furnace-quenched. (B) Room temperature X-ray diffraction (XRD) pattern of the quenched product, showing the major phase of $Bi_{25}FeO_{39}$, with minor amounts of Fe_2O_3 (unreacted starting material), and the first appearance of product $BiFeO_3$.

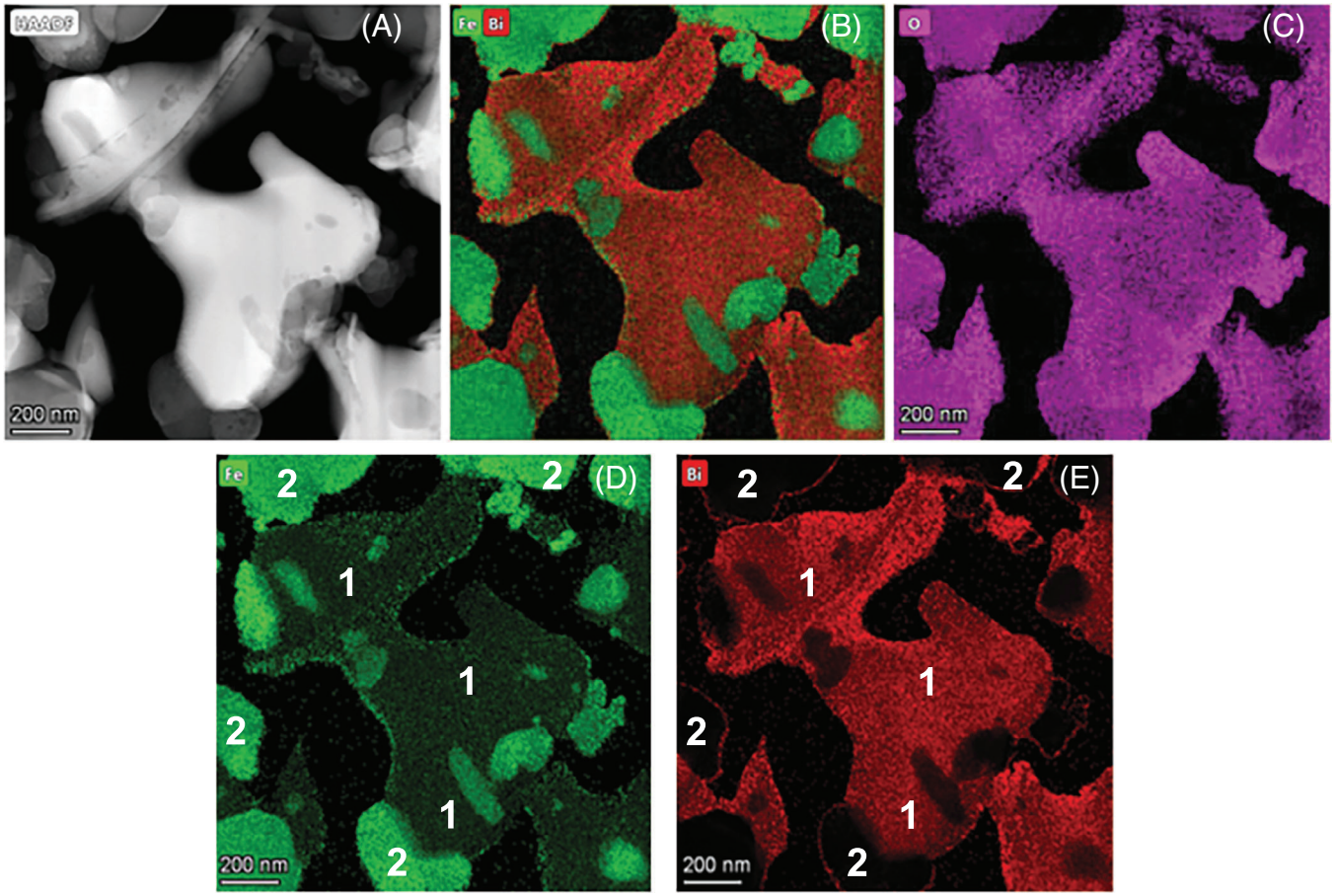

FIGURE 6 Transmission electron microscopy (TEM) image and energy-dispersive spectroscopy (EDS) maps of the equimolar Bi_2O_3 and Fe_2O_3 mixture that was heated to 650°C and then quenched in order to examine the intermediate phase. High-angle annular dark field (HAADF) in (A), combined Fe and Bi chemical map in (B), O map in (C), Fe map in (D), and Bi map in (E). In parts (D) and (E), two types of particles are identified, 1 and 2, which correspond to the sillenite phase and remaining Fe_2O_3, respectively.

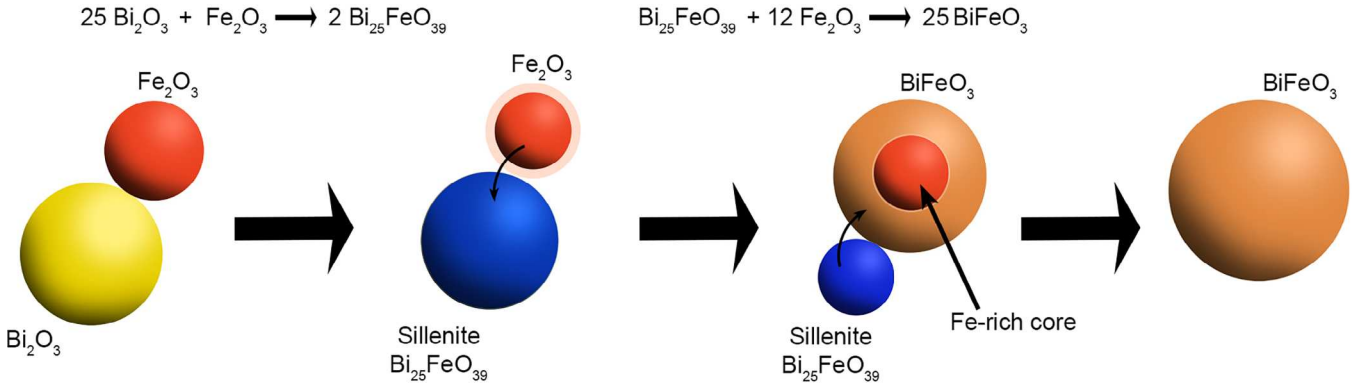

FIGURE 7 Schematic diagram illustrating the reaction sequence of Bi_2O_3 and Fe_2O_3 during the formation of $BiFeO_3$.

4 | CONCLUSIONS

Collectively, these experiments demonstrate that the reaction of Bi_2O_3 with Fe_2O_3 to form $BiFeO_3$ occurs through an intermediate phase; specifically, the Bi_2O_3 transforms to $Bi_{25}FeO_{39}$ through the incorporation of a small fraction of the Fe_2O_3. It is emphasized that all the Bi_2O_3 transforms to $Bi_{25}FeO_{39}$. Thus, $Bi_{25}FeO_{39}$ is not only present due to the chemical gradients innate to Bi_2O_3 and Fe_2O_3 interdiffusion[4] and from thermodynamic decomposition from $BiFeO_3$;[1,13] in addition, $Bi_{25}FeO_{39}$ forms as an intermediate compound in the reaction that further reacts with remaining Fe_2O_3 to form $BiFeO_3$. The reaction sequence in the solid-state synthesis of $BiFeO_3$ is illustrated in Figure 7. Sillenite $Bi_{25}FeO_{39}$ is indicated as an intermediate phase that reacts with the remainder of the Fe_2O_3 to yield $BiFeO_3$. Given these new insights that $Bi_{25}FeO_{39}$ is inevitably formed during the synthesis of $BiFeO_3$, continuing studies can focus on other factors such as the purity of the starting materials, the Bi:Fe stoichiometry, and the particle sizes.

In summary, the experiments demonstrate that sillenite $Bi_{25}FeO_{39}$ occurs as an intermediate product of Bi_2O_3 and a small amount of Fe_2O_3. All the Bi_2O_3 reacts to form sillenite $Bi_{25}FeO_{39}$, which then reacts with the remaining Fe_2O_3 to form the product $BiFeO_3$. Therefore, the synthesis of perovskite $BiFeO_3$ is shown to occur via a two-step reaction sequence with $Bi_{25}FeO_{39}$ as an intermediate compound.

ACKNOWLEDGMENTS

This work was supported by the National Science Foundation (NSF), as part of the Center for Dielectrics and Piezoelectrics under grant nos. IIP-1841453 and IIP-1841466. This work was performed at the Analytical Instrumentation Facility (AIF) at North Carolina State University and at the NC State Nanofabrication Facility (NNF), both of which are supported by the State of North Carolina and the National Science Foundation (Award No. ECCS-2025064). AIF and NNF are members of the North Carolina Research Triangle Nanotechnology Network (RTNN), a site in the National Nanotechnology Coordinated Infrastructure (NNCI). Dr. Alexandra Goodnight is acknowledged for redrawing Figure 1 and creating Figure 7, Darrell Harry for assistance with the SEM experiments, and Dr. Chris Winkler for assistance with the TEM experiments.

ORCID

Corrado Wesley https://orcid.org/0000-0001-6964-7265
Elizabeth C. Dickey https://orcid.org/0000-0003-4005-7872
Jacob L. Jones https://orcid.org/0000-0002-9182-0957

REFERENCES

1. Rojac T, Bencan A, Malic B, Tutuncu G, Jones JL, Daniels JE, et al. $BiFeO_3$ ceramics: processing, electrical, and electromechanical properties. J Am Ceram Soc. 2014;97(7):1993–2011.
2. Selbach SM, Einarsrud M-A, Tybell T, Grande T. Synthesis of $BiFeO_3$ by wet chemical methods. J Am Ceram Soc. 2007;90(11):3430–34.
3. Xu J-H, Ke H, Jia D-C, Wang W, Zhou Y. Low-temperature synthesis of $BiFeO_3$ nanopowders via a sol-gel method. J Alloys Compd. 2009;472:473–77.
4. Bernardo MS, Jardiel T, Peiteado M, Caballero AC, Villegas M. Reaction pathways in the solid state synthesis of multiferroic $BiFeO_3$. J Eur Ceram Soc. 2011;31:3047–53.
5. Palai R, Katiyar RS, Schmid H, Tissot P, Clark SJ, Robertson J, et al. β phase and γ-β metal-insulator transition in multiferroic $BiFeO_3$. Phys Rev. 2008;B77:014110.
6. Valant M, Axelsson A-K, Alford N. Peculiarities of a solid-state synthesis of multiferroic polycrystalline $BiFeO_3$. Chem Mater. 2007;19(22):5431–36. https://doi.org/10.1021/cm071730
7. Morozov MI, Lomanova NA, Gusarov V. Specific features of $BiFeO_3$ formation in a mixture of bismuth(III) and iron(III) oxides. Russ J Gen Chem. 2003;73(11):1676–80.
8. Thrall M, Freer R, Martin C, Azough F, Patterson B, Cernik RJ. An in situ study of the formation of multiferroic bismuth ferrite

using high resolution synchrotron X-ray powder diffraction. J Eur Ceram Soc. 2008;28(13):2567–72.
9. Rao CNR, Subba Rao GV, S Ramdas S. Phase transformations and electrical properties of bismuth sesquioxide. J Phys Chem. 1969;73:672–75.
10. Hull S. Superionics: crystal structures and conduction processes. Rep Prog Phys. 2004;67:1233–314.
11. Harwig HA, Gerards AG. The polymorphism of bismuth sesquioxide. Thermochim Acta. 1979;28:121–31.
12. Selbach SM, Einarsrud M-A, Grande T. On the thermodynamic stability of $BiFeO_3$. Chem Mater. 2009;21:169–173.
13. Salazar-Pérez AJ, Camacho-López MA, Morales-Luckie RA, Sánchez-Mendieta V, Ureña-Núñez F, Arenas-Alatorre J. Structural evolution of Bi_2O_3 prepared by thermal oxidation of bismuth nano-particles. Superf y Vacío. 2005;18(3):4–8.
14. Jebari H, Tahiri N, Boujnah M, El Bounagui O, Taibi M, Ez-Zahraouy H. Theoretical investigation of electronic, magnetic and magnetocaloric properties of $Bi_{25}FeO_{40}$ compound. Phase Transit. 2021;94(3–4):147–58.
15. Levin EM, Roth RS. Polymorphism of bismuth sesquioxide. II. Effect of oxide additions on the polymorphism of Bi_2O_3. J Res Natl Bur Stand A. 1964;68A:197–206.
16. Levin EM, Roth RS. Polymorphism of bismuth sesquioxide. I. Pure Bi_2O_3. J Res Natl Bur Stand A. 1964;68A:189–95.

SUPPORTING INFORMATION

Additional supporting information can be found online in the Supporting Information section at the end of this article.

How to cite this article: Wesley C, Bellcase L, Forrester JS, Dickey EC, Reaney IM, Jones JL. Solid state synthesis of $BiFeO_3$ occurs through the intermediate $Bi_{25}FeO_{39}$ compound. J Am Ceram Soc. 2024;1–8. https://doi.org/10.1111/jace.19702